

Dynamic effective mass of granular media

Chaur-Jian Hsu¹, David L. Johnson¹, Rohit A. Ingale², John J. Valenza¹, Nicolas Gland², and Hernán A. Makse²

¹*Schlumberger-Doll Research, One Hampshire Street, Cambridge, MA 02139*

²*Levich Institute and Physics Department, City College of New York, New York, NY 10031*

(Dated: March 23, 2022)

We develop the concept of frequency dependent effective mass, $\tilde{M}(\omega)$, of jammed granular materials which occupy a rigid cavity to a filling fraction of 48%, the remaining volume being air of normal room condition or controlled humidity. The dominant features of $\tilde{M}(\omega)$ provide signatures of the dissipation of acoustic modes, elasticity and aging effects in the granular medium. We perform humidity controlled experiments and interpret the data in terms of a continuum model and a “trap” model of thermally activated capillary bridges at the contact points. The results suggest that attenuation in the granular materials studied here can be influenced significantly by the kinetics of capillary condensation between the asperities at the contacts.

PACS: 45.70.-n, 46.40.-f, 81.05.Rm

A distinct feature of jammed or loosely packed granular materials made of a variety of different materials such as sand, steel, polymer or glass is the ability to dissipate acoustic energy through the network of interparticle contacts or viscous dissipation through the surrounding medium. Indeed, loose grains damp acoustic modes very efficiently [1–5] and they are routinely used as an effective method to optimize the damping of unwanted structure-borne acoustic signals [1]. Despite its fundamental importance and practical applications, the microscopic origins of the mechanisms of dissipation in jammed granular materials are still unknown.

In this Letter, we pursue the concept of a frequency dependent effective mass, $\tilde{M}(\omega)$, of a loose granular aggregate contained within a rigid cavity [5]. The effective mass $\tilde{M}(\omega)$ is complex valued; its real part reflects the inertial and elastic properties while its imaginary part reflects the dissipative properties of the granular medium. We demonstrate how the features of $\tilde{M}(\omega)$ allow the study of some of the mechanisms of damping of acoustic modes, aging and elasticity in granular matter.

Generally speaking, the real part of $\tilde{M}(\omega)$ exhibits a sharp resonance which we interpret in terms of an effective sound speed. The imaginary part of $\tilde{M}(\omega)$ shows a broad resonance peak which quantifies the attenuation of acoustic waves in the system. We observe significant changes in the stiffness and attenuation as a function of humidity. By monitoring the effective mass in time, we find a logarithmic aging effect in the resonance frequency as well as an increase of the damping upon humidification. These effects can be modeled as capillary condensation occurring between the asperities at the contact surfaces between the grains during humidity-dry cycles. We interpret this phenomenon in the context of a “trap model” of thermally activated liquid bridges. Our results suggest that, in the granular materials investigated in the present study, dissipation of acoustic energy is dominated by the asperities at the interparticle contact surfaces. In addition, humidity drastically affects the attenuation of the material through the capillary condensation of liquid bridges.

Experiments.— A cylindrical cavity (of diameter $D=25.4$ mm) excavated in a rigid aluminum cup is filled with tungsten particles up to a height of 30.7 mm. We use tungsten particles due to their large density, which maximizes the effects we are studying. Each of these particles consists of four or five equal-axis particles, of nominal size $100\text{ }\mu\text{m}$, fused together (see inset of Fig. 1). Such irregular arrangement produces low volume fractions (in this case 48%, in comparison with random close packing of spherical particles, 64%) and allows to study the loose packings of interest in the present work. To investigate the applicability of our results to other materials we perform experiments with spherical glass beads as well as lead beads, see below. The cup is mounted on a B&K shaker and subjected to a vertical sinusoidal vibration at frequency $\omega = 2\pi f$, with the frequency scan from sub kHz to 10 kHz. Since the bulk behavior depends on the contacts between the grains, the way of filling the gran-

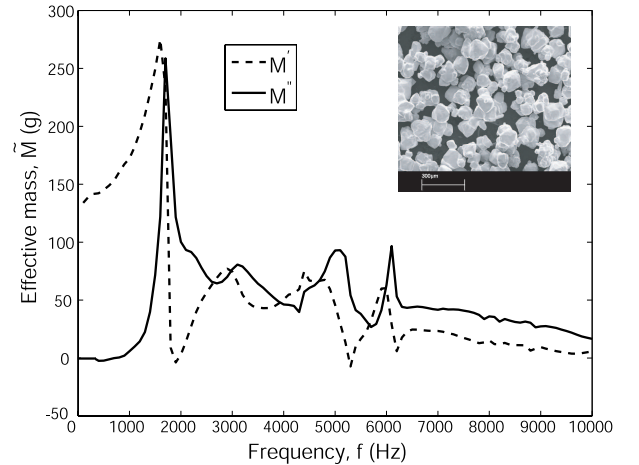


FIG. 1: Effective mass of tungsten particles in a rigid cavity as a function of driving frequency. Inset: Scanning Electron Microscope image of the tungsten particles used in our experiments. The scale at the bottom of the image corresponds to $300\mu\text{m}$.

ular medium in the container is important. Prior to the measurement, we pour the grains into the cup and then shake the cup near its resonance frequency (see below) at large amplitudes up to 3g for 30 minutes to allow the compaction of the material. During the measurement, the granular medium is driven with cup acceleration of approximately 2 to 3 ms^{-2} . The amplitude of vibration is approximately 1 μm for the lower frequencies and decreases to below 1 nm for the higher frequencies.

Force $F(\omega)$ and acceleration $a(\omega)$ are independently measured with a force gauge and an accelerometer attached to the bottom of the cup. The signals are analogically filtered with a lock-in amplifier, which is synchronized with the driving signal. These filtered signals are then digitally recorded. The force gauge is sandwiched between the shaker and the cup container. At each frequency, the force and acceleration are averaged over a 500 ms or longer time window. Prior to this time window, there is a 3 sec waiting time following the onset of the driving frequency in order to allow the system to reach a steady state, and achieve accurate measurements. Since $F(\omega)$ and $a(\omega)$ are the net force exerted on and the response of the cup-granules assembly, their ratio, the effective mass, is independent of the shakers frequency response. Taking into account the mass of the empty cup, M_c , we have $\tilde{M}(\omega) + M_c = \frac{F(\omega)}{a(\omega)}$, where, $\tilde{M}(\omega) \equiv M'(\omega) + iM''(\omega)$, reflects the partially in-phase, M' , partially out-of-phase, M'' , motion of the individual grains, relative to the driving force. Thus M' carries information about the inertia and elastic response while M'' relates to attenuation of particle response.

Fig. 1 shows the result for a frequency sweep of $\tilde{M}(\omega)$. We note that in the low frequency limit, $M'(\omega \rightarrow 0) \rightarrow 149g$, the static mass of the grains. More interestingly, there is a relatively sharp resonance peak around $f_0 \equiv \omega_0/2\pi = 1.8$ kHz and a relatively broad tail that diminishes with increasing frequency. M'' exhibits a broad peak centered at ω_0 . We have conducted the experiments with other granular materials. Fig. 2(a)-(b) shows the results for spherical lead beads of the size 180-250 μm and glass beads of 150 μm . These results are qualitatively similar to those of tungsten particles, in both the real and imaginary parts; the tungsten particles exhibit larger effects.

We also applied the effective mass technique to liquid samples. Fig. 2c shows a typical plot for the effective mass of one such liquid (fluorocarbon fluid, density 1800 kg/m^3) as measured by the effective mass technique. $M'(\omega)$ shows a sharp resonance while the $M''(\omega)$ curve is almost zero over the whole frequency range (except near resonance) indicating negligible dissipation. We can extract a value for the effective compressional sound speed from the resonance frequency as $v_s(L) = 4Lf_0$, where L is the depth of the medium. The values of density and sound speed for a variety of liquids, as measured with the effective-mass technique, are cross-plotted against those determined by more conventional means [6] in Fig. 2d.

The density of the liquids is measured using Archimedes principle and buoyancy (accuracy of 0.1%). The sound speed is measured with ultrasonic (centered at 500 kHz) through-transmission method (accuracy of 1%). The grain density of the tungsten sample is measured with a Micromeritics helium pycnometer (accuracy 1%) and the bulk density is calculated from the measured weight of tungsten grains filling a cup of a known volume. Volume fraction is then estimated from the grain and bulk density. The results in Fig. 2d suggests that our technique for measuring $\tilde{M}(\omega)$ is an accurate one.

We investigate how the effective sound speed changes with the filling depth L , based on the peak frequency f_0 . The sound speed of the granular media is estimated based on the hypothesis of 1/4 wavelength resonance frequency. Fig. 2e shows the trend of greater speed with greater depth. The values we are reporting are of the same order of magnitude as those reported in the literature [1, 3, 5, 7]. In the range studied here, the linear relation $v_s(L) \sim L$ seems to hold up to $L = 61$ mm as seen in Fig. 2e.

We may model the general features of Fig. 1 in terms of a simplified continuum model. The granular

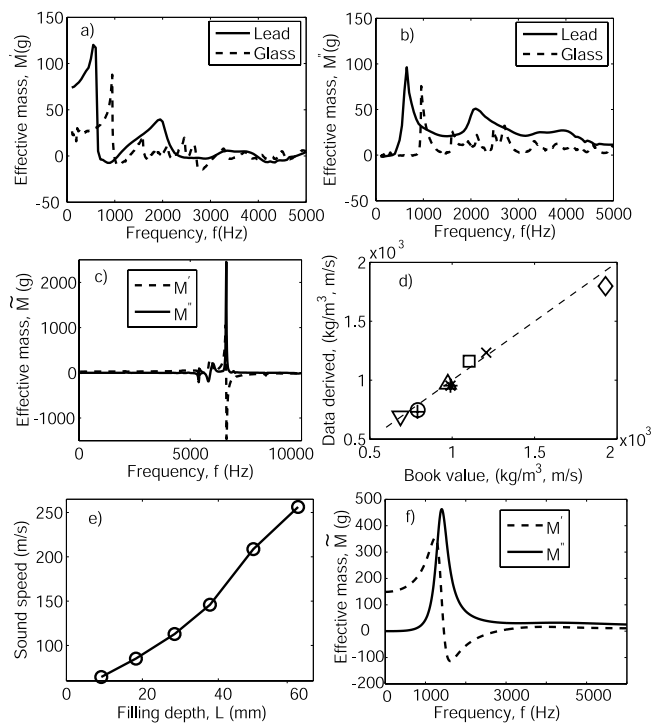


FIG. 2: (a) Real (M') and (b) Imaginary part (M'') of effective mass for spherical lead and glass beads. (c) Effective mass of fluorocarbon fluid. (d) Crossplot of measured values and book values of densities and sound speeds for various liquids: Methanol (o and \square , first symbol density, second sound speed), Ethanol (+ and \times), Fluorocarbon fluid (\diamond and ∇), Silicon oil, (viscosity 10 mPa-s, \triangle and $*$). (e) Effective speed of sound in tungsten granules as a function of filling depth, L , for constant cavity diameter, $D = 25.4$ mm. (f) Continuum model prediction of $\tilde{M}(\omega)$.

medium is considered to be a lossy fluid, with negligible viscous effects at the walls. The acoustic pressure in the fluid is described by a one-dimensional model: $P(z) = A \sin(qz) + B \cos(qz)$. The boundary conditions are: (a) The displacement of the fluid at $z = 0$ matches that of the cup, $u(z = 0) = u_{\text{cup}}$. (b) The acoustic pressure at the top of the fluid vanishes, $P(z = L) = 0$. Thus, $P(z) = u_{\text{cup}} \rho \omega^2 [\sin(qz) - \tan(qL) \cos(qz)]/q$. The force the cup exerts on the fluid is $F = \pi a^2 P(z = 0)$ and the acceleration of the cup is $-\omega^2 u_{\text{cup}}$ from which we obtain the effective mass:

$$\tilde{M}(\omega) = \pi a^2 \sqrt{\rho K} / \omega \tan(qL), \quad (1)$$

where $K = K_0[1 - i\omega\xi]$ is the (lossy) bulk modulus of the medium, and $q = \omega \sqrt{\rho/K}$ is the complex wave vector with ρ the density of the medium. This model shows that resonance peaks, as seen in Fig. 2f, occur when L equals odd multiples of $1/4$ wavelength of the acoustic wave in the medium, with the main resonance peak at $f_0 = 1/(4L) \sqrt{K_0/\rho}$. Encouraged by these results, we interpret the main resonance in Fig. 1 as being a $1/4$ wavelength resonance of the compressional sound speed.

Next, we use the features in $\tilde{M}(\omega)$ to investigate the dissipation in the granular medium. The dissipation mechanisms can be grouped into two categories: 1) Local damping throughout the contact network that includes asperity deformation and bulk attenuation [8], and wetting dynamics in the liquid bridges caused by relative motion of neighboring particles [9]. Wetting dynamics also results in greater contact stiffness [10]. If large inter-particle tangential displacements occur then, there exist dissipation through Coulomb friction as well. 2) Global damping due to drag caused by particle motion in a surrounding viscous medium [11].

Next, we perform further experimentation by changing the ambient conditions. Ambient humidity can modify the dissipation and the stiffness at the grain to grain surface contacts [10]. For instance, small amounts of liquid greatly affects the maximum angle of stability in sand-piles [12], while capillary action of the interstitial liquid results in increased cohesion [10], modified friction [13] and aging in the angle of repose of granular materials [14]. We place the effective mass apparatus in a chamber where humidity is controlled by first using an aqueous saturated salt solution [15] and subsequently a dessicant. We measure the relative humidity as the ratio of the partial pressure of water to the saturating vapor pressure $H_R = p_{\text{vap}}/p_{\text{sat}}$.

We follow a humid-dry cycling process as follows: we start from room humidity $H_R = 26\%$ at $t < 0$, and then we humidify at $t = 0$ to $H_R = 75\%$ until $t = 126$ hr, and then we dry to $H_R = 0\%$ until $t = 174$ hr. Fig. 3 shows the effective mass measurements under the humidity controlled environment carried out at various time intervals. We observe a very slow shift in resonant frequency during the humidification cycle, followed by a further positive shift upon drying. The effect is more important when we repeat the same cycling but to 95% humidity.

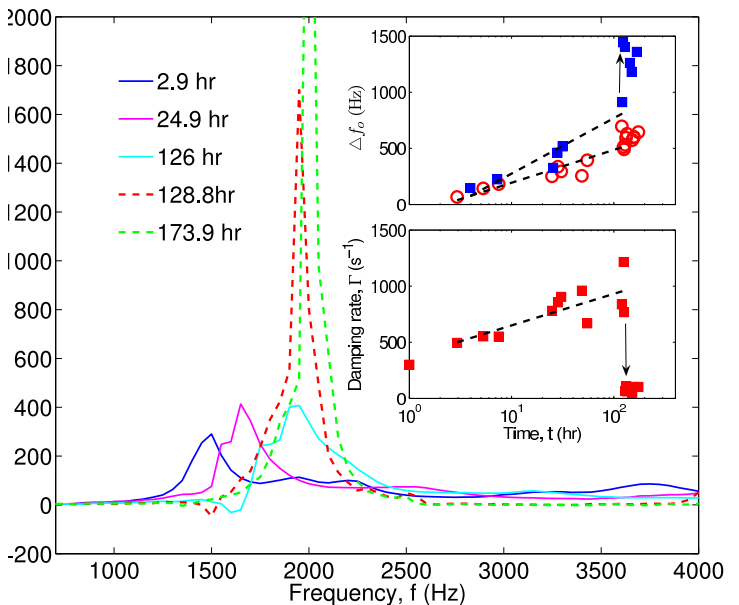


FIG. 3: Imaginary part of $\tilde{M}(f)$ measured under humidity controlled conditions (the real part shows similar behavior). The solid lines represent measurements under $H_R = 75\%$ and the dashed lines are for the dry state, $H_R = 0\%$. Top inset: Frequency shift vs time for $H_R = 75\%$ (o) and 95% (□). Bottom inset: Damping rate (Γ) vs time for $H_R = 75\%$. The dashed lines in the insets are logarithmic fits. The up and down arrows indicates the large variations in stiffness and damping upon drying, respectively.

During humidification, we observe an aging phenomenon as evidenced by the approximate logarithmic behavior of the shift in resonant frequency $\Delta f_0(t)$ (top inset of Fig. 3), $\Delta f_0(t) = C(H_R) \log(t/t_i)$, where $C(H_R)$ is a constant that increases with humidity, $C(75\%) = 292$ Hz and $C(95\%) = 494$ Hz and $t_i \approx 2$ hr for both measures.

Furthermore, the humid system shows a large increase in the attenuation as illustrated by the increase in damping rate Γ (bottom inset of Fig. 3). Based on the experimental effective mass data, we search for poles in $\tilde{M}(\tilde{\omega})$ for $\tilde{\omega}$ in the complex plane. Once the complex resonance frequency ($\tilde{\omega}_0 = \omega'_0 + i\omega''_0$) is found, the damping rate is given by $\Gamma = -\omega''_0$. The damping rate at ambient humidity is 300 s^{-1} , which rises to 1200 s^{-1} under prolonged humidification (see bottom inset of Fig. 3). The damping data suggests logarithmic increase with time.

A possible interpretation of the observed behavior suggests that contact forces through capillary liquid bridges are important for damping, stiffness and aging. As demonstrated in [14], the humidification process leads to the formation of capillary bridges around the roughness asperities at the interparticle contact surfaces. The aging effect observed in the logarithmic variation of the frequency shift with time can be interpreted as originating from capillary condensation. The key quantity to calculate is the time dependence of the number of wetted

asperities $n_a(t)$. Capillary condensation at the surface asperities can be seen as a thermally activated process following a model proposed in [14]. The energy barrier to form a liquid bridge of cross sectional area A between two asperities separated by a gap h is $\Delta E = \Delta\mu\rho_l Ah$, where ρ_l is the molecular density of the condensing liquid, $\Delta\mu = k_B T \ln(1/H_R)$ is the undersaturation of the chemical potential, and T the room temperature. The activation process follows an Arrhenius dynamics such that the time to create a bridge is $\tau = t_0 \exp(\Delta E/k_B T)$, with t_0 the microscopic condensation time.

Due to the roughness of the particles we expect a distribution of gaps $P(h)$, which leads to a distribution of energy barriers, $P(\Delta E)$. The calculation of the probability distribution $P(\tau)$ is then analogous to obtaining the probability of the time to escape from a trap with energy barrier ΔE for a thermally activated particle in a random energy potential. Such a process corresponds to the “trap model” used to describe the phenomenology of glasses [16]. The probability $P(\tau)$ satisfies $P(\tau)d\tau = P(h)dh$. While the probability $P(h)$ is unknown, we expect it to be a bounded distribution determined by the surface roughness of the particles. The two most common cases lead to the same result: for an exponential or Gaussian distribution of gaps, we find $P(\tau) \sim \tau^{-1}$.

The number of activated wetted asperities at time t is $n_a(t) \propto \int_{t_0}^t P(\tau)d\tau$. Then $n_a(t) \approx \log(t/t_0)$. Liquid bridges induce a significant cohesion between the particles which for loose grains under gravity and large humidity outweigh the weight of the grains. Therefore, the logarithmic increase in n_a leads to an additional stiffness with the concomitant increase in the compressional sound speed. Since the resonance frequency is proportional to the stiffness of the contact, the logarithmic aging can be interpreted as arising from the wetted asperities.

Upon drying the particles to $H_R = 0\%$ after humidification, the physics is very different from the humid process. As shown by the experiments of [10], the capillary

rings dry out and the asperities are sucked down by the increasing capillary pressure in the evaporating film leading to an even larger increase in stiffness of the contacts. Thus, in the dried out state there is much more solid on solid contact and the sound speed is increased. This increase in stiffness upon drying results in even larger positive shifts in resonant frequency as seen in the top inset of Fig. 3.

We also find important changes in the dissipation in the dry state. Upon drying, the decrease in overall attenuation is evident from the much sharper resonance in M'' (we find a very large mass at resonance $M''(f_0) \approx 3500$ g). Accordingly, the damping rate decreases to $\Gamma = 50$ s^{-1} in the dry case from $\Gamma = 1200$ s^{-1} at $H_R = 75\%$ (see bottom inset of Fig. 3). In the driest state, no liquids bridges are left and the dissipation is purely through asperities deformation with the concomitant lower damping strength. These results suggest that, for the granular media studied here when humid conditions prevail (including ambient), liquid bridges provide larger attenuation of acoustic waves than the viscoelastic dissipation in the bulk of the particles or viscous global damping.

In conclusion, we have demonstrated the usefulness of the effective mass technique to study the dissipation of acoustic waves, stiffness and aging in granular media. Experiments and theoretical models suggest that capillary condensation at the interparticle contacts is an important mechanism for dissipation and aging. The kinetics of aging can be modeled in terms of a trap model for the formation of liquid bridges at the asperities. The large variations in dissipation found in this study demonstrate the conditions for effective particle damping and are relevant to a variety of applications for optimizing attenuation of structure-borne acoustic waves.

Acknowledgments. We are grateful to L. McGowan for technical assistance. We acknowledge financial support from DOE, Geosciences Division.

-
- [1] L. Cremer and M. Heckl, *Structure Borne Sound* (Springer, Berlin, 1973).
 - [2] J. Duran, *Sands, powders and grains. An introduction to the physics of granular materials* (Springer-Verlag, 2000).
 - [3] C.-h. Liu and S. Nagel, *Phys. Rev. Lett.* **68**, 2301 (1992).
 - [4] J. M. Bourinet and D. Le Houedec, *Computers and Structures* **73**, 395 (1999).
 - [5] J. M. Bourinet and D. Le Houedec, *Powders & Grains 97* eds. R. Behringer and J. Jenkins (Balkema, Rotterdam, 1997).
 - [6] Handbook of Chemistry and Physics, 81st Edition (CRC Press, Cleveland, 2000).
 - [7] F. D. Shields, J. M. Sabatier and M. Wang, *J. Acoust. Soc. Am.* **108**, 1998 (2000).
 - [8] N. V. Brilliantov, F. Spahn, J.-M. Hertzsch, and T. Pöschel, *Phys. Rev E* **53**, 5382 (1996).
 - [9] J. Crassous, E. Charlaix, H. Gayvallet, and J.-L. Loubet, *Langmuir* **9**, 1995 (1993); J. Crassous, E. Charlaix, and J.-L. Loubet, *Phys. Rev. Lett* **78**, 2425 (1997); M. J. Adams and V. Perchard, *Inst. Chem. Engr. Symp.* **91**, 147 (1985).
 - [10] J. N. D'Amour, *et al. Phys. Rev. Lett.* **96**, 058301 (2006).
 - [11] J. Schäfer, S. Dippel, and D. E. Wolf, *J. Phys. I (France)* **6**, 5 (1996).
 - [12] D. J. Hornbaker, R. Albert, I. Albert, A.-L. Barabási, P. Schiffer, *Nature* **387**, 765 (1997).
 - [13] E. Riedo, F. Lévy, and H. Brune, *Phys. Rev. Lett.* **88**, 185505 (2002).
 - [14] L. Bocquet, E. Charlaix, S. Ciliberto and J. Crassous, *Nature* **396**, 735 (1998).
 - [15] F. Restagno, C. Ursini, H. Gayvallet, and E. Charlaix, *Phys. Rev. E* **66**, 021304 (2002).
 - [16] C. Monthus and J.-P. Bouchaud, *J. Phys. A* **29**, 3847 (1996).